

CREEP STRESSES IN FUNCTIONALLY GRADED ROTATING ORTHOTROPIC CYLINDER WITH VARYING THICKNESS AND DENSITY UNDER INTERNAL AND EXTERNAL PRESSURE

NAPONI PUZANJA U ROTIRAJUĆEM ORTOTROPNOM CILINDRU OD FUNKCIONALNIH KOMPOZITA PROMENLJIVE DEBLJINE I GUSTINE PRI UNUTRAŠNJEM I SPOLJNOM PRITISKU

Originalni naučni rad / Original scientific paper

UDK /UDC: 62-988:539.3/4

66-988:539.3/4

Rad primljen / Paper received: 27.04.2018

Adresa autora / Author's address:

Department of Mathematics, Jaypee Inst. of Inform. Technology, Noida (UP), India email: sanjit12@rediffmail.com

Keywords

- creep
- orthotropic
- functionally graded material
- pressure
- cylinder
- variable thickness
- variable density
- temperature

Abstract

Effects of material inhomogeneity on creep stresses in a functionally graded cylinder with thickness and density variations have been investigated. Analysis is performed by means of transition theory using the concept of generalized strain measure. Analytical solution for an orthotropic cylinder subjected to pressure and temperature is derived. The results indicate that the effect of material inhomogeneity and nonlinearity of measure is very pronounced. Highly non-homogeneous isotropic material steel with nonlinear measure is safer for the design as compared to orthotropic materials barite and uranium (alpha) as generated circumferential stresses are lower in steel as compared to barite and uranium.

INTRODUCTION

In the past two decades, widespread attention has been given to anisotropic materials in industry. Therefore, the analysis of anisotropic material structure is quite complicated. Increased use of orthotropic materials in engineering applications leads to extensive research activity in these types of anisotropic materials. The functionally graded material whose composition and properties change in a certain direction plays a vital role in the design of a composite structure (Noda et al. /1/, and Sokolnikoff /2/). Rotating cylinders have various applications i.e. steam and gas turbines, speed cameras, planetary landing, composite rotors etc. In the application of composite rotors, the cylinder must operate under severe mechanical and thermal loading that causes creep, and hence reduces the service life. The high creep strength together with high specific strength offered by functionally graded material poses an acceptable selection for these applications. The analysis of such functionally graded rotating orthotropic cylinders has been reported scarcely in literature. Creep stress analysis of isotropic cylinder under pressure has been discussed by (King /3/, Pai et al. /4/, and Bhatnagar et al. /5/) using

Ključne reči

- puzanje
- ortotropan
- funkcionalni kompozitni materijali
- pritisak
- cilindar
- promenljiva debljina
- promenljiva gustina
- temperatura

Izvod

Istražen je uticaj nehomogenosti materijala na napone puzanja u cilindru promenljive debljine i gustine, izrađen od funkcionalnog kompozitnog materijala. Analiza je obuhvatila primenu teorije prelaznih napona sa konceptom generalisane mere deformacija. Izvedeno je analitičko rešenje za ortotropni cilindar pod dejstvom pritiska i temperature. Rezultati ukazuju na izraženi uticaj nehomogenosti materijala i nelinearnost mera deformacija. Čelični nehomogeni izotropni materijal sa nelinearnim merama deformacija se pokazuje kao sigurniji u projektovanju u poređenju sa ortotropnim materijalima baritom i uranijumom (alfa), jer su generisani periferni naponi niži kod čelika nego kod ovih materijala.

assumptions like infinitesimal deformation theory, creep strain law etc. Experimental and theoretical study was performed by King et al. on thick-walled cylinder subjected to internal pressure. Pai et al. /4/ emphasizes on the influence of material anisotropy in creep behaviour of the structure under loading. Bhatnagar et al. /5/ calculated creep strains using the Norton law. Also, steady state creep stresses were investigated by Hoseini et al. /6/ in thick-walled pressurized rotating shells using Norton's law with plane strain condition in order to demonstrate the effect of angular speed on stress. An analytical solution for creep stresses in thick functionally graded rotating cylindrical pressure vessels under steady state has been obtained by Nejad et al. /7/, and they concluded that the property of functionally graded material has significant effect on the stresses in pressure vessels. Later (Pai /4/, Bhatnagar et al. /8/ and Gupta et al. /9/) solved the problem of orthotropic cylinders. Nowinski /10/ generalized the Galerkin's problem to an orthotropic tube subjected to any axi-symmetric temperature field. Thermal stresses in a non-homogeneous hollow orthotropic rotating cylinder are investigated by Naggat et al. /11/ using finite difference method and concluded that orthotropy has significant influence on stresses.

Dag /12/ developed a new computational method based on the generalized definition of the J-integral to study crack problems in orthotropic functionally graded materials under thermal stresses. Also, Sharma et al. /13/ investigated thermal stresses in rotating functionally graded stainless steel composite cylinder under internal and external pressure using finite difference method. Analytical solutions obtained by all these authors considered yield criterion, linear strain measure, jump conditions, using the concept of infinitesimal strain theory. The drawback of the classical theory is that it cannot provide the solution for the physical problem for finite deformation. To overcome this, Seth /14/ introduced the transition theory. Sharma et al. /15/ presented an analytical solution for thermal creep stresses in non-homogeneous thick walled cylinder under internal and external pressure using transition theory. Sharma et al. /16/ investigated thermal plastic stresses for a transversely isotropic thick-walled rotating cylinder under pressure and concluded that circular cylinder rotating under pressure made up of isotropic material is on the safer side of the design as compared to circular cylinder made up of transversely isotropic material. Aggarwal et al. /17/ analysed the effect of pressure on cylinder made up of transversely isotropic material beryl and isotropic material steel, and concluded that beryl is good for designing purposes as the pressure required for initial yielding to become fully plastic is higher in beryl. Sharma /20/ investigated thermal elastic-plastic stresses in thick-walled circular cylinder under internal and external pressure, while Sharma /21/ discussed creep stresses in bending of functionally graded plate using the concept of transition theory with the use of generalized strain measure.

This present paper deals with creep behaviour in thick-walled rotating functionally graded orthotropic cylinder with variable thickness and density subjected to pressure and temperature.

FORMULATION OF THE PROBLEM

We consider the non-homogeneous hollow cylinder with inner and outer radii r_i and r_o respectively, made up of orthotropic material rotating at angular velocity ω about its centre. We consider the case of axi-symmetric deformations so that only displacement component is u_r . The z -axis is the axis of rotation. The non-homogeneity in the cylinder is due to variation of compressibility C . In cylindrical polar coordinates, the displacements are given as:

$$u_r = r(1 - \beta), \quad u_\theta = 0 \quad \text{and} \quad u_z = dz, \quad (1)$$

where: β is a function of r ; and d is a constant.

We assume the non-homogeneity in the elastic constants C_{ij} of the form

$$C_{ij} = C_{0ij} \left(\frac{r}{r_0} \right)^{-k}, \quad (2)$$

where: k is the non-homogeneity parameter.

The thickness and density of the cylinder are assumed to vary along the radius in the form

$$\rho = \rho_0 \left(\frac{r}{r_0} \right)^{-q}, \quad h = h_0 \left(\frac{r}{r_0} \right)^{-t}, \quad (3)$$

where: q and t are gradient parameters.

The generalized principal strain measure defined by Seth /18/ is given as

$$e_{ii} = \int_0^{e_{ii}^A} [1 - 2e_{ii}^A]^{\frac{n-1}{2}} de_{ii}^A = \frac{1}{n} \left[1 - (1 - 2e_{ii}^A)^{\frac{n}{2}} \right] \quad (i = 1, 2, 3), \quad (4)$$

where: n is strain measure; and e_{ii}^A are the principal Almansi finite components of strain.

The generalized components of strain are given as

$$\begin{aligned} e_{rr} &= \frac{1}{n} [1 - (r\beta' + \beta)^n], \quad e_{\theta\theta} = \frac{1}{n} [1 - \beta^n], \\ e_{zz} &= \frac{1}{n} [1 - (1-d)^n], \quad e_{r\theta} = e_{\theta z} = e_{zr} = 0. \end{aligned} \quad (5)$$

The thermal stress-strain relations (Naggar 2002, /11/) are given by

$$\begin{aligned} \sigma_{rr} &= C_{11}e_{rr} + C_{12}e_{\theta\theta} + C_{13}e_{zz} - \beta_1 T, \\ \sigma_{\theta\theta} &= C_{21}e_{rr} + C_{22}e_{\theta\theta} + C_{23}e_{zz} - \beta_2 T, \\ \sigma_{zz} &= C_{31}e_{rr} + C_{32}e_{\theta\theta} + C_{33}e_{zz} - \beta_3 T, \\ \sigma_{\theta z} &= C_{44}e_{\theta z}, \\ \sigma_{zr} &= C_{55}e_{zr}, \\ \sigma_{r\theta} &= C_{66}e_{r\theta}, \end{aligned} \quad (6)$$

where: $\beta_1 = C_{11}\alpha_r + C_{12}\alpha_\theta + C_{13}\alpha_z$; $\beta_2 = C_{21}\alpha_r + C_{22}\alpha_\theta + C_{23}\alpha_z$; $\beta_3 = C_{31}\alpha_r + C_{32}\alpha_\theta + C_{33}\alpha_z$, where α_i are the thermal expansion coefficients and C_{ij} are elastic constants.

Using Eq.(5) in Eq.(6) we get

$$\begin{aligned} \sigma_{rr} &= \frac{C_{11}}{n} [1 - (r\beta' + \beta)^n] + \frac{C_{12}}{n} [1 - \beta^n] + \frac{C_{13}}{n} [1 - (1-d)^n] - \beta_1 T, \\ \sigma_{\theta\theta} &= \frac{C_{21}}{n} [1 - (r\beta' + \beta)^n] + \frac{C_{22}}{n} [1 - \beta^n] + \frac{C_{23}}{n} [1 - (1-d)^n] - \beta_2 T, \\ \sigma_{zz} &= \frac{C_{31}}{n} [1 - (r\beta' + \beta)^n] + \frac{C_{32}}{n} [1 - \beta^n] + \frac{C_{33}}{n} [1 - (1-d)^n] - \beta_3 T, \\ \sigma_{r\theta} &= \sigma_{\theta z} = \sigma_{zr} = 0. \end{aligned} \quad (7)$$

Equations of equilibrium are all satisfied except

$$\frac{d}{dr} (hr\sigma_{rr}) - h\sigma_{\theta\theta} + h\rho\omega^2 r^2 = 0. \quad (8)$$

where: r is the radial coordinate; σ_{rr} and $\sigma_{\theta\theta}$ are the radial and circumferential stresses respectively; h is the cylinder thickness; and ρ is the material density of the rotating non-homogeneous cylinder.

IDENTIFICATION OF TRANSITION POINT

In response to applied loading to a deformable solid, it has been observed that the solid first deforms elastically. If the loading is sustained, plastic flow might set in and lead to creep. So, there exists an intermediate state in between elastic and creep state which is known as transition state. In order to clarify the transition from elastic to creep state, firstly, we need to identify transition state as an asymptotic one. Thus, the differential system defining the elastic state should reach a critical value in the transition state. The non-linear differential equation for transition state is obtained by substituting Eq.(7) in Eq.(8) as

$$\frac{d\beta}{dP} \left[hP(P+1)^n + \frac{C_{012} \left(\frac{r}{b}\right)^{-k}}{C_{011} \left(\frac{r}{b}\right)^{-k}} hP - \frac{\rho\omega^2 r^2 h}{nC_{011} \left(\frac{r}{b}\right)^{-k} \beta^n} + \frac{h}{nC_{011} \left(\frac{r}{b}\right)^{-k} \beta^n} \left[\left\{ (k+t-1)C_{011} \left(\frac{r}{b}\right)^{-k} + C_{021} \left(\frac{r}{b}\right)^{-k} \right\} \{1-\beta^n(P+1)^n\} + \right. \right. \tag{9}$$

$$\left. \left. + \left\{ (k+t-1)C_{012} \left(\frac{r}{b}\right)^{-k} + C_{022} \left(\frac{r}{b}\right)^{-k} \right\} \{1-\beta^n\} + \left\{ (k+t-1)C_{013} \left(\frac{r}{b}\right)^{-k} + C_{023} \left(\frac{r}{b}\right)^{-k} \right\} \{1-(1-d)^n\} \right] + h\beta P(P+1)^{n-1} \right] = 0,$$

where: $r\beta' = P\beta$.

The critical points of β in Eq.(9) are $P \rightarrow 0$, $P \rightarrow -1$, and $P \rightarrow \pm\infty$.

The boundary conditions are

$$\sigma_{rr} = -p_1 \text{ at } r = r_i \text{ and } \sigma_{rr} = -p_2 \text{ at } r = r_o. \tag{10}$$

The resultant normal force to plane $Z = const.$ must $R_1 = \sigma_{rr} - \sigma_{\theta\theta} = \frac{1}{n} [(C_{11} - C_{21})\{1 - \beta^n(P+1)^n\} + (C_{12} - C_{22}) \times$

$$\times \{1 - \beta^n\} + (C_{13} - C_{23})\{1 - (1-d)^n\} + (\beta_2 - \beta_1)nT] \tag{11}$$

STRESSES

It has been shown, Borah /19/, that transition function through the stress-difference at the transition point $P \rightarrow -1$, yield creep stresses. We define the transition function R_1 as

$$R_1 = \sigma_{rr} - \sigma_{\theta\theta} = \frac{1}{n} [(C_{11} - C_{21})\{1 - \beta^n(P+1)^n\} + (C_{12} - C_{22}) \times \tag{12}$$

Taking logarithmic differentiation of Eq.(12) with respect to 'r', and taking the asymptotic value as $P \rightarrow -1$, and integrating, we get

$$R_1 = AF_1, \tag{13}$$

where: A is constant of integration; $F_1 = e^{\int Xdr}$; and

$$X = \frac{1}{r} \left[\left(\frac{C_{11} - C_{21}}{C_{11}} \right) (-kC_{11}r^n - nD^n C_{12} - n\rho\omega^2 r^{n+2} + r^n \{ (k+t-1)C_{11} + C_{21} \} + \{ (k+t-1)C_{12} + C_{22} \} \{ r^n - D^n \} + r^n \{ (k+t-1)C_{13} + C_{23} \} + \right. \tag{14}$$

$$\left. \frac{(C_{11} - C_{21})r^n + (C_{12} - C_{22})\{r^n - D^n\} + r^n(C_{13} - C_{23})\{1 - (1-d)^n\} + \{1 - (1-d)^n\} + (C_{12} - C_{22})\{nD^n - kr^n + kD^n\} + (C_{13} - C_{23})\{-kr^n + kr^n(1-d)^n\}}{(C_{11} - C_{21})r^n + (C_{12} - C_{22})\{r^n - D^n\} + r^n(C_{13} - C_{23})\{1 - (1-d)^n\} + \{1 - (1-d)^n\} + (C_{12} - C_{22})\{nD^n - kr^n + kD^n\} + (C_{13} - C_{23})\{-kr^n + kr^n(1-d)^n\}} \right] + (\beta_2 - \beta_1)nT_0 \log r$$

Using Eq.(13) in Eq.(12), we get

$$\sigma_{rr} - \sigma_{\theta\theta} = AF_1. \tag{14}$$

Using Eq.(14) in equilibrium equation, we get

$$\sigma_{rr} = AF(r) - \frac{\rho\omega^2 r^2}{2-(t+q)} + B, \tag{15}$$

$$\sigma_{\theta\theta} = \sigma_{rr} - AF_1, \tag{16}$$

where: $F(r) = \frac{1}{h} \int \frac{hF_1}{r} dr$, $\sigma_{zz} = \frac{C_{32}(\sigma_{rr} + \sigma_{\theta\theta})}{C_{12} + C_{22}} + A_1$, $\tag{17}$

where:

$$A_1 = \left\{ C_{31} - \frac{C_{32}(C_{11} + C_{21})}{C_{12} + C_{22}} \right\} + \left\{ C_{33} - \frac{C_{32}(C_{13} + C_{23})}{C_{12} + C_{22}} \right\} e_{zz}.$$

Using boundary condition from Eq.(10) in Eq.(15), we get

$$A = \frac{p_2 - p_1 - \frac{\rho\omega^2(r_o^2 - r_i^2)}{2-(t+q)}}{\int_{r_i}^{r_o} Fdr},$$

$$B = -p_2 + \frac{p_2 - p_1 - \frac{\rho\omega^2(r_o^2 - r_i^2)}{2-(t+q)}}{\int_{r_i}^{r_o} Fdr} F(r_o) + \frac{\rho\omega^2 r_o^2}{2-(t+q)}.$$

Putting the values of A and B in Eqs.(15-16), the creep stresses for the orthotropic cylinder are given by

$$\sigma_{rr} = -p_2 + \frac{\left\{ (p_1 - p_2) + \frac{\rho\omega^2(r_o^2 - r_i^2)}{2-(t+q)} \right\} \int_r^{r_o} Fdr}{\int_{r_i}^{r_o} Fdr} + \frac{\rho\omega^2 r_o^2}{2-(t+q)} \tag{18}$$

$$\sigma_{\theta\theta} = -p_2 + \frac{\left\{ (p_1 - p_2) + \frac{\rho\omega^2(r_o^2 - r_i^2)}{2-(t+q)} \right\} \left[\int_r^{r_o} Fdr + e^{\int Xdr} \right]}{\int_{r_i}^{r_o} Fdr} + \tag{19}$$

$$+ \frac{\rho\omega^2(r_o^2 - r^2)}{2-(t+q)}.$$

Introducing the following non-dimensional components as $R = (r/r_o)$, $R_0 = (r_i/r_o)$, $T_{rr} = [\sigma_{rr}/C_{011}]$, $T_{\theta\theta} = [\sigma_{\theta\theta}/C_{011}]$,

$$T_{zz} = [\sigma_{zz}/C_{011}], \Omega^2 = \frac{\rho\omega^2 r_o^2}{C_{011}}.$$

The radial, circumferential and axial creep stresses given by Eqs.(15-17) in non-dimensional form for functionally graded orthotropic cylinder can be rewritten as

$$T_{rr} = -P_2 + \left\{ P_1 - P_2 + \frac{\Omega^2(1-R_0^2)}{2-(t+q)} \right\} \frac{\int_R^1 F_2 dR}{\int_{R_0}^1 F_2 dR} + \frac{\Omega^2(1-R^2)}{2-(t+q)}, \quad (20)$$

where: $F_2(r) = \frac{1}{h} \int \frac{hF_1}{r_o R} e^{r_o \int X_1 dR} dR$ and

$$X_1 = \frac{1}{r_o R} \left(\frac{C_{11}-C_{21}}{C_{11}} \right) \left(-kC_{11} - \frac{nD^n}{r_o^n R^n} C_{12} - n\rho\omega^2 r_o^2 R^2 + \{(k+t-1)C_{11}+C_{21}\} + \{(k+t-1)C_{12}+C_{22}\} \left\{ 1 - \frac{D^n}{r_o^n R^n} \right\} + \{(k+t-1)C_{13}+C_{23}\} \{1-(1-d)^n\} \right) + \frac{(C_{11}-C_{21})+(C_{12}-C_{22}) \left\{ 1 - \frac{D^n}{r_o^n R^n} \right\} + r^n (C_{13}-C_{23}) \{1-(1-d)^n\} + (C_{12}-C_{22}) \left(\frac{nD^n}{r_o^n R^n} - k \left\{ 1 - \frac{D^n}{r_o^n R^n} \right\} \right) - k(C_{13}-C_{23}) \{1-(1-d)^n\}}{+(\beta_2 - \beta_1) T_0 n \log R},$$

$$T_{\theta\theta} = -P_2 + \left\{ P_1 - P_2 + \frac{\Omega^2(1-R_0^2)}{2-(t+q)} \right\} \frac{\int_R^1 F_2 dR}{\int_{R_0}^1 F_2 dR} \left[\int_R^1 r_o F_2 dR + e^{r_o \int X_2 dR} \right] + \frac{\Omega^2(1-R^2)}{2-(t+q)}, \quad (21)$$

$$T_{zz} = \frac{C_{32}(T_{rr}+T_{\theta\theta})}{C_{12}+C_{22}} + \left\{ C_{31} - \frac{C_{32}(C_{11}+C_{21})}{C_{12}+C_{22}} \right\} + \left\{ C_{33} - \frac{C_{32}(C_{13}+C_{23})}{C_{12}+C_{22}} \right\} e_{zz}. \quad (22)$$

For homogeneous orthotropic cylinder with uniform thickness, density and without thermal effects, these stresses are same as that obtained by Gupta et al. /8/.

NUMERICAL DISCUSSION AND RESULTS

In this study, creep stress is analysed on a hollow cylinder of functionally graded material (FGM) by using an analytic solution with plain strain assumption. Inner and outer radii of the cylinder are taken as $r_i = 1$ and $r_o = 2$, respectively. Mechanical property of the cylinder, such as compressibility, density, thickness and temperature are assumed to vary through the radius. The material property of the orthotropic and isotropic cylinder made of FGM is given in Table 1.

The parameters of thermal expansion coefficient for orthotropic material are considered as: $\alpha_r = 40 \times 10^{-6}$, $\alpha_\theta = 10 \times 10^{-6}$ and $\alpha_z = 40 \times 10^{-6}$, and for the isotropic material as $\alpha_r = \alpha_\theta = \alpha_z = 15 \times 10^{-6}$. To observe the influence of various parameters i.e. temperature, $\bar{T}_0 = T_0 / \log R_0$; strain measure $N = 1/n$; and pressure P_1 and P_2 on thick-walled circular cylinder made up of functionally graded material (barite, uranium and steel), Table 1 and graphs have been drawn between radii ratio and creep stresses for various pressure and thickness combinations under centrifugal force. Results are given in non-dimensional form. When the thick-walled cylinder is pressurized, the bore material which is an extremely stressed portion of the cylinder - begins to yield. The yield surface starts to propagate through the thickness of the cylinder until it reaches the outer surface.

In Figs. 1-8, presented is the variation of hoop stresses along the radial direction of the cylinder subjected to uniform temperature load $T_0 = 0.05$, for different gradient parameters. Hoop stresses decrease gradually from inner to outer surface for negative non-homogeneity parameters. The highly non-homogeneous cylinder is having lower circumferential creep stresses on the contrary to the cylinder of less non-homogeneous material, as seen in Figs. 1-8. The stresses are maximal at the inner surface and tensile in nature. It has been noticed from Fig. 1 that creep stresses are maximal for uranium as compared to barite and steel. It has also been observed that with the decrease in non-homogeneity parameter ($k = -1$ to $k = -5$), circumferential creep stresses increase significantly. It has been noticed from Figs. 1 and 2 that with the increase in nonlinearity measure ($N = 3$ to 9) the circumferential creep stress decreases. The dots and solid lines in Figs. 1-8 represent the results for thickness gradient parameter $t = -1, -1.5$.

It has been observed from Figs. 1 and 3 that with the decrease in angular speed, hoop stresses decrease significantly for rotating cylinder of orthotropic and isotropic material. The effect of temperature and nonlinearity on the stresses can be seen from Tables 2, 3 and 4. Circumferential creep stresses decrease with the introduction of thermal effect, but the deformation is negligible. Introduction of nonlinearity of strain measure indicates considerable change in creep stresses, because in the case of classical theory, nonlinear transition region via which yield occurs is overlooked while creep stresses are never linear.

Table 1. Elastic constants C_{ij} used (in units of 10^{11} N/m²).

Materials	C11	C12	C13	C21	C22	C23	Density
steel (isotropic material)	5.326	3.688	3.688	3.688	5.326	3.688	7.849
barite (orthotropic material)	0.8941	0.4614	0.2691	0.4614	0.7842	0.2676	4.4
uranium (alpha) (orthotropic material)	2.1486	0.4622	0.2176	0.4622	1.9983	1.0764	19.04

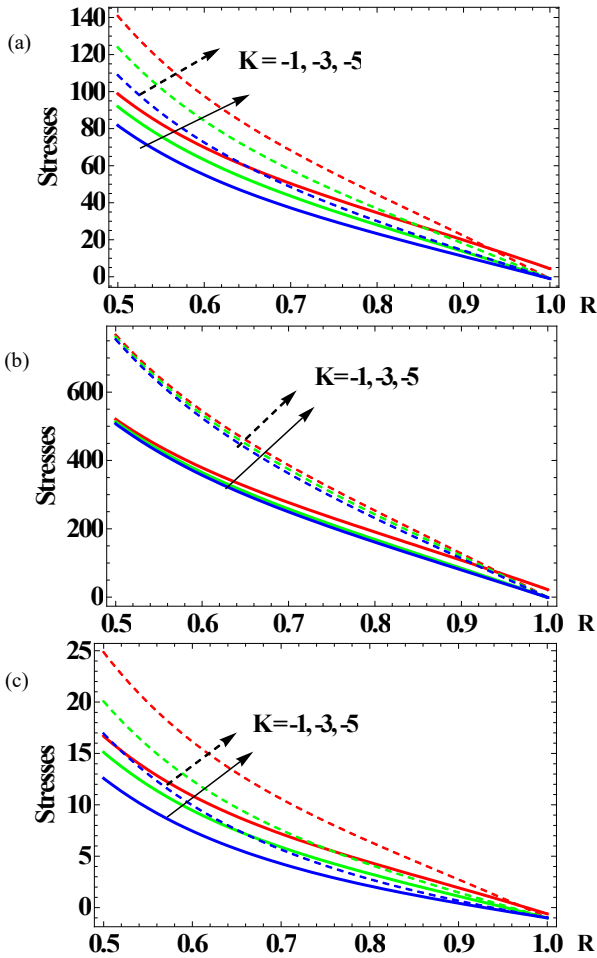


Figure 1. Creep stresses for different materials: (a) barite; (b) uranium (alpha); (c) steel, with $P_1 = 1.5, P_2 = 1, \Omega^2 = 1, \bar{T}_0 = 0.05, N = 3$, and variable thickness parameter t , where dashed and solid lines represent $t = -1, -1.5$ in respect.

It can be seen from Fig. 4 that with the increase in nonlinearity of measure, creep stress decreases. With the change in measure from linear to nonlinear, circumferential stresses decrease significantly as can be seen from Tables 2, 3 and 4. Also, the circumferential creep stress is maximal for less non-homogeneous rotating cylinder as compared to highly non-homogeneous rotating cylinder. Out of two orthotropic materials i.e. barite and uranium, lower circumferential stresses are generated for barite as compared to uranium. With the increase in angular speed, these stresses increase significantly as can be seen from Tables 2, 3 and 4. Figures 5-8 show the effect of increasing internal pressure on the hoop stresses. Figures 5-8 have been drawn with internal pressure $P_1 = 9.5$ and external pressure $P_2 = 1$. With increase in internal pressure, circumferential stresses increase as can be seen from Figs. 5-8 and these stresses are tensile in nature. Also, Figs. 7c and 8c show circumferential creep stresses that are lower for isotropic material steel with thickness gradient parameters $t = -1.5$, as compared to thickness gradient parameters $t = -1$. Also, steel is having lower circumferential stresses as compared to orthotropic materials barite and uranium. There is a noticeable increase in the hoop stress with the decrease in wall thickness. It can

be seen from Figs. 1 to 8 that creep stresses are lower for high value of thickness gradient parameter.

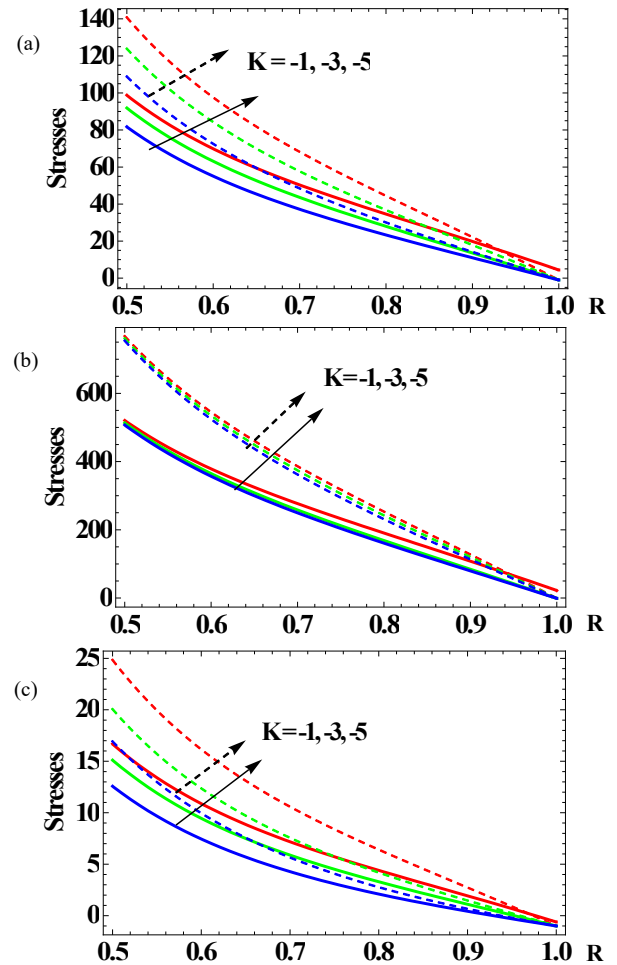
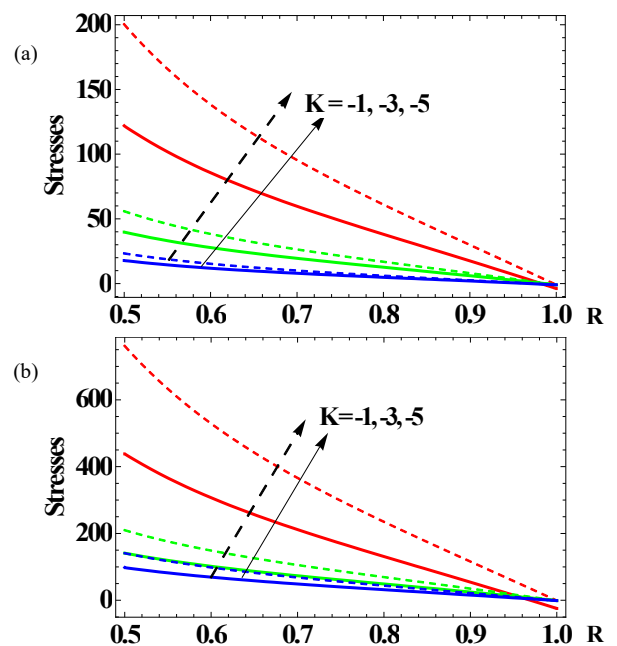


Figure 2. Creep stresses for different materials: (a) barite; (b) uranium (alpha); (c) steel, with $P_1 = 1.5, P_2 = 1, \Omega^2 = 1, \bar{T}_0 = 0.05, N = 9$, and variable thickness parameter t , where dashed and solid lines represent $t = -1, -1.5$ in respect.



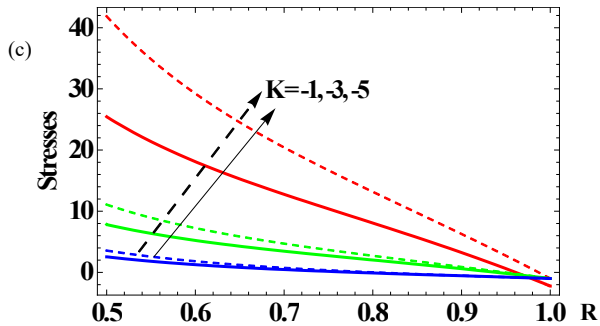


Figure 3. Creep stresses for different materials: (a) barite; (b) uranium (alpha); (c) steel, with $P_1 = 1.5, P_2 = 1, \Omega^2 = 0.5, \bar{T}_0 = 0.05, N = 3$, and variable thickness parameter t , where dashed and solid lines represent $t = -1, -1.5$ in respect.

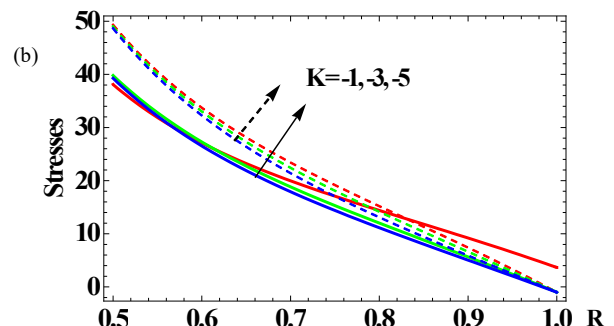
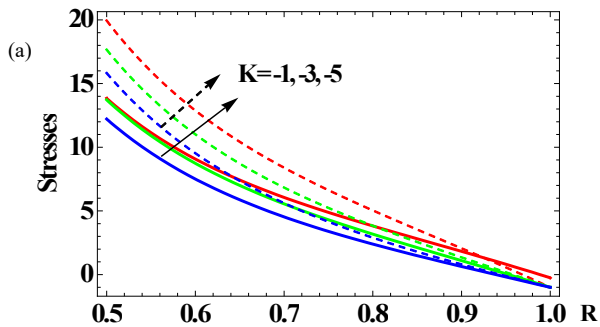


Figure 4. Creep stresses for different materials: (a) barite; (b) uranium (alpha); (c) steel, with $P_1 = 1.5, P_2 = 1, \Omega^2 = 0.5, \bar{T}_0 = 0.05, N = 9$, and variable thickness parameter t , where dashed and solid lines represent $t = -1, -1.5$ in respect.

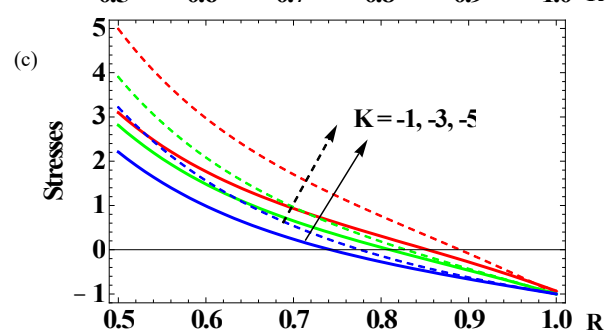


Figure 4. Creep stresses for different materials: (a) barite; (b) uranium (alpha); (c) steel, with $P_1 = 1.5, P_2 = 1, \Omega^2 = 0.5, \bar{T}_0 = 0.05, N = 9$, and variable thickness parameter t , where dashed and solid lines represent $t = -1, -1.5$ in respect.

Table 2. Circumferential creep stresses for rotating cylinder of barite with linear- $N = 1$ and nonlinear strain hardening measure $N = 3$.

Barite (without thermal effects)													
Measure		Linear						Nonlinear					
Angular velocity		0.7			1.4			0.7			1.4		
Pressure	R/k	-1	0	1	-1	0	1	-1	0	1	-1	0	1
$P_1 = 10$	0.5	492.2	424.2	273.6	19879.9	21524.7	22560	80.7	82.4	79.3	2412.5	2437.2	2443.7
	0.6	363.4	300.8	202.3	13977.9	14230.2	14258.6	57.3	57.4	53.8	1707.9	1709.6	1698.4
$P_2 = 5$	0.7	268.4	209.3	140.2	9786.1	9265.1	8760	40.9	39.9	36.1	1203.4	1192.5	1172.9
	0.8	183.5	132.7	85.6	6344	5544.6	4890.2	26.8	25.2	21.9	784.1	769	748.5
Barite (with thermal effects)													
Measure		Linear						Nonlinear					
Angular velocity		0.7			1.4			0.7			1.4		
Pressure	R/k	-1	0	1	-1	0	1	-1	0	1	-1	0	1
$P_1 = 10$	0.5	492.1	424.2	273.68	19878.2	21523.3	22559	80.7	82.4	79.2	2412.5	2437.1	2443.67
	0.6	363.4	300.8	202.35	13976.7	14229.3	14257.9	57.3	57.4	53.8	1707.8	1709.5	1698.4
$P_2 = 5$	0.7	183.5	209.3	140.23	9785.3	9264.5	8759.5	40.9	39.9	36.1	1203.3	1192.5	1172.89
	0.8	95.4	132.7	85.56	6343.6	5544.4	4889.9	26.8	25.2	21.8	784.1	769	748.55

Table 3. Circumferential creep stresses for rotating cylinder of uranium with linear- $N = 1$ and nonlinear strain hardening measure $N = 3$.

Uranium (without thermal effects)													
Measure		Linear						Nonlinear					
Angular velocity		0.7			1.4			0.7			1.4		
Pressure	R/k	-1	0	1	-1	0	1	-1	0	1	-1	0	1
$P_1 = 10$	0.5	5953.2	6216.8	5817.6	313100	363714	407789	758.8	802.7	758.2	33375.3	33993.6	34280.7
	0.6	4075.8	4008.5	3670.5	206783	223153	236730	545.4	567.8	527.1	23115.8	23428.9	23512.1
$P_2 = 5$	0.7	2760.6	2504.1	2180.5	134820	133030	131262	390.9	399.9	364.2	15905.6	16036.2	16009.4
	0.8	1724.3	1416.8	1142.4	80952.9	71985.3	64800.1	259.1	260.3	232.3	10117.9	10146.5	10075.8
Uranium (with thermal effects)													
Measure		Linear						Nonlinear					
Angular velocity		0.7			1.4			0.7			1.4		
Pressure	R/k	-1	0	1	-1	0	1	-1	0	1	-1	0	1
$P_1 = 10$	0.5	5953.2	6216.8	5817.6	313099	363714	407789	758.8	802.7	758.1	33375.3	33993.6	34280.6
	0.6	4075.8	4008.5	3670.5	206783	223153	236730	545.3	567.8	527.1	23115.8	23428.9	23512.1
$P_2 = 5$	0.7	2760.6	2504.1	2180.5	134820	133030	131262	390.8	399.9	364.2	15905.6	16036.2	16009.3
	0.8	1724.3	1416.8	1142.4	80952.9	71985.3	64800.1	259.1	260.3	232.3	10117.7	10146.5	10075.8

Table 4. Circumferential creep stresses for rotating cylinder of steel with linear- $N = 1$ and nonlinear strain hardening measure $N = 3$.

Steel (without thermal effects)													
Measure		Linear						Nonlinear					
Angular velocity		0.7			1.4			0.7			1.4		
Pressure	R/k	-1	0	1	-1	0	1	-1	0	1	-1	0	1
$P_1 = 10$	0.5	197.5	59.7	20.4	547.7	458.3	346.2	111.7	25.9	4.9	380.3	127.9	62.39
	0.6	164.5	50.5	14.5	593.8	386.1	253.8	86.6	18.5	1.5	274.9	91.3	42.08
$P_2 = 5$	0.7	162.5	45.1	10.3	657.3	332.8	186.4	67.2	13.2	-0.6	199.5	65.8	28.54
	0.8	154.4	37.8	6.4	639.4	266.4	126.7	47.9	8.3	-2.1	134.5	43.9	17.59

Steel (with thermal effects)													
Measure		Linear						Nonlinear					
Angular velocity		0.7			1.4			0.7			1.4		
Pressure	R/k	-1	0	1	-1	0	1	-1	0	1	-1	0	1
$P_1 = 10$	0.5	197.5	59.7	20.4	547.7	458.3	346.2	111.7	25.9	4.9	380.3	127.9	62.4
	0.6	164.5	50.5	14.5	593.8	386	253.9	86.6	18.5	1.5	274.9	91.3	42.1
$P_2 = 5$	0.7	162.5	45.1	10.3	657.3	332.8	186.4	67.2	13.2	-0.63	199.5	65.8	28.5
	0.8	154.4	37.8	6.35	639.4	266.4	126.7	47.9	8.3	-2.14	134.5	43.9	17.6

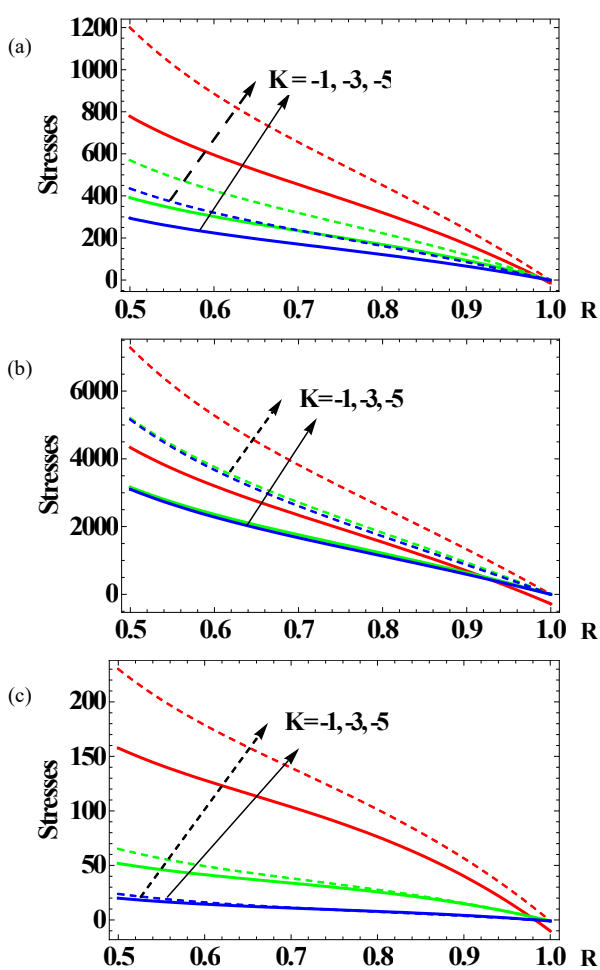


Figure 5. Creep stresses for different materials: (a) barite; (b) uranium (alpha); (c) steel, with $P_1 = 9.5, P_2 = 1, \Omega^2 = 1, \bar{T}_0 = 0.05, N = 3$, and variable thickness parameter t , where dashed and solid lines represent $t = -1, -1.5$ in respect.

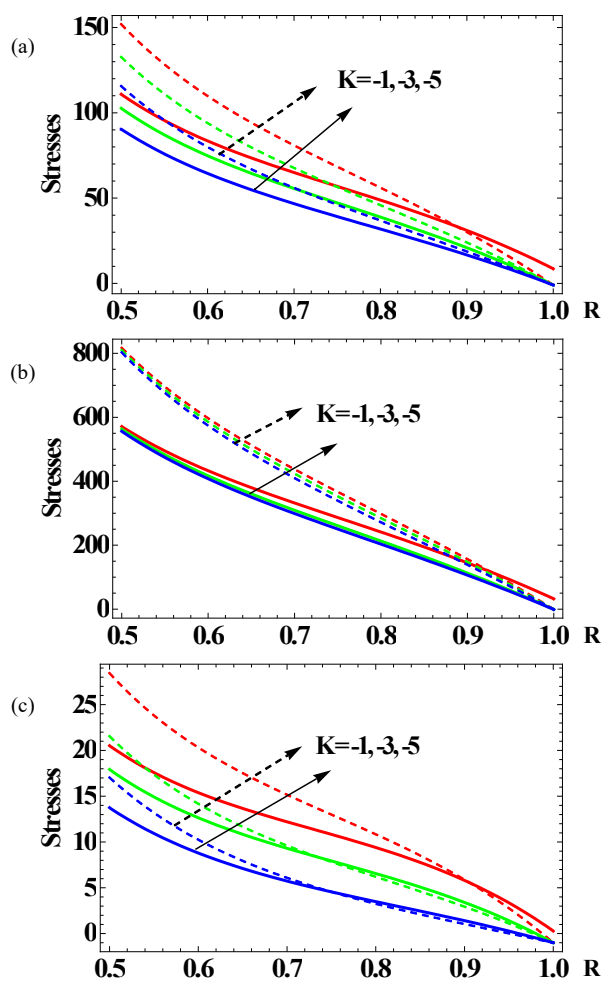


Figure 6. Creep stresses for different materials: (a) barite; (b) uranium (alpha); (c) steel, with $P_1 = 9.5, P_2 = 1, \Omega^2 = 1, \bar{T}_0 = 0.05, N = 9$, and variable thickness parameter t , where dashed and solid lines represent $t = -1, -1.5$ in respect.

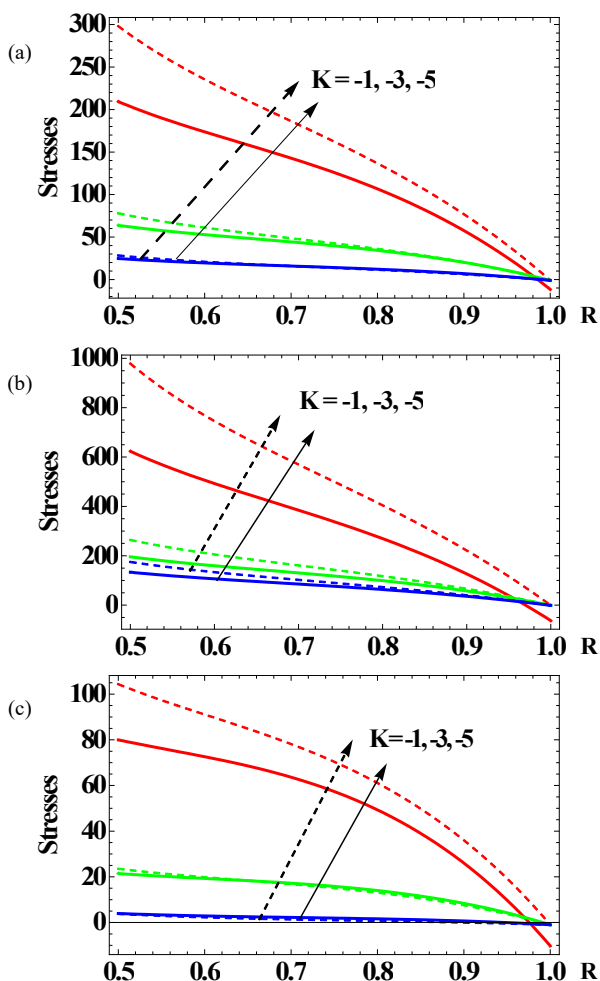


Figure 7. Creep stresses for different materials: (a) barite; (b) uranium (alpha); (c) steel, with $P_1 = 9.5, P_2 = 1, \Omega^2 = 0.5, \bar{T}_0 = 0.05, N = 3$, and variable thickness parameter t , where dashed and solid lines represent $t = -1, -1.5$ in respect.

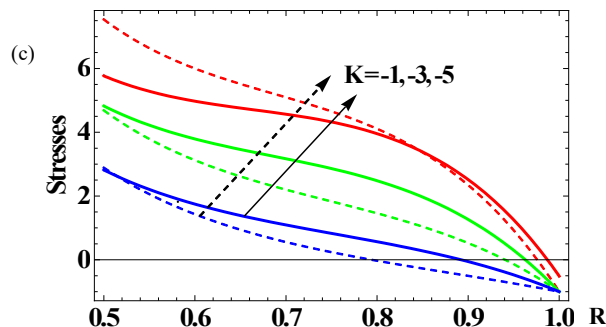
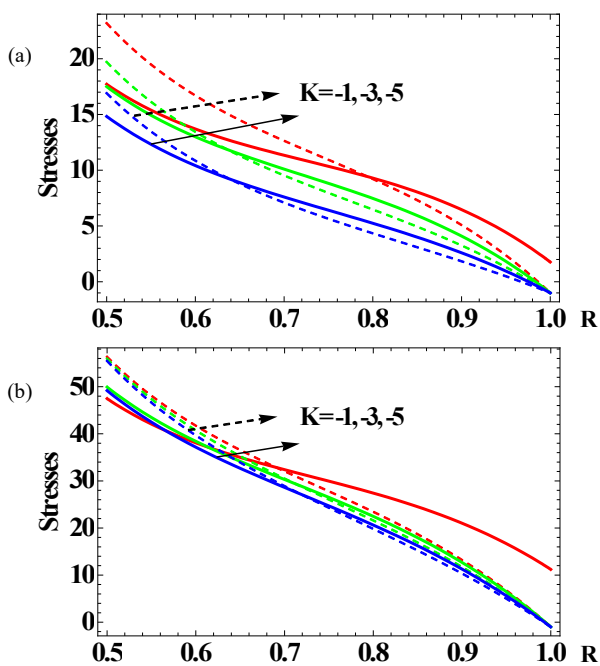


Figure 8. Creep stresses for different materials: (a) barite; (b) uranium (alpha); (c) steel, with $P_1 = 9.5, P_2 = 1, \Omega^2 = 0.5, \bar{T}_0 = 0.05, N = 9$, and variable thickness parameter t , where dashed and solid lines represent $t = -1, -1.5$ in respect.

CONCLUSION

In this paper, creep stresses in radial, circumferential and axial direction for rotating pressurized functionally graded cylinder with varying thickness and density are determined. The results indicate that the effect of inhomogeneity is very pronounced. Effect of inhomogeneity is studied for orthotropic and isotropic material. Highly non-homogeneous isotropic material steel with nonlinear measure is safer for the design as hoop stress generated is lower in case of steel as compared to barite and uranium. Among orthotropic materials, highly functionally graded barite is a better orthotropic material for the choice of design as compared to uranium (alpha), as circumferential creep stresses generated for the cylinder made of barite are lower. Also, the cylinder whose thickness increases radially, and density decreases radially is on the safer side of design.

REFERENCES

1. Noda, N., Hetnarski, R.B., Tanigawa, Y. (2002), Thermal Stresses, CRC Press.
2. Sokolnikoff, I.S. (1956), Mathematical Theory of Elasticity, 2nd ed., McGraw-Hill.
3. King, R.H., Mackie, W.W. (1967), *Creep of thick-walled cylinders*, ASME J Basic Eng., 89(4): 877-884.
4. Pai, D.H., (1967), *Steady state creep analysis of thick-walled orthotropic cylinders*, Int. J Mech. Sci., 9(6): 335-348. doi.org/10.1016/0020-7403(67)90039-2
5. Bhatnagar, N.S., Kulkarni, P., Arya, V.K. (1986), *Analysis of an orthotropic thick-walled cylinder under primary creep conditions*, Int. J Press. Ves. and Piping, 23(3): 165-185.
6. Hoseini, Z., Nejad, M.Z., Niknejad, A., Ghannad, M. (2011), *New exact solution for creep behavior of rotating thick-walled cylinders*, J Basic Appl. Sci. Res., 1(10): 1704-1708.
7. Nejad, M.Z., Hoseini, Z., Taghizadeh, T., Niknejad, A. (2013), *Closed-form analytical solution for creep stresses of pressurized functionally graded material thick spherical shells*, Adv. Sci. Lett., 19(2): 464-467.
8. Bhatnagar, N.S., Gupta, S.K. (1969), *Analysis of thick-walled orthotropic cylinder in the theory of creep*, J Phys. Soc. Jpn., 27: 1655-1661.
9. Gupta S.K., Bhardwaj P.C. (1986), *Elastic-plastic and creep transition in an orthotropic rotating cylinder*, Proc. Indian Natn. Sci. Acad., 52(6a): 1357-1369.
10. Nowinski, J. (1957), *Thermoelastic states in a thick-walled orthotropic cylinder surrounded by an elastic medium*, Bull. l' Académie Polonaise Sci. (BAPMAM), 5: 19-22.

11. El-Naggar, A.M., Abd-Alla, A.M., Fahmy, M.A., Ahmed, S.M. (2002), *Thermal stresses in a rotating non-homogeneous orthotropic hollow cylinder*, Heat & Mass Transfer, 39(1):41-46.
12. Dag, S. (2006), *Thermal fracture analysis of orthotropic functionally graded materials using an equivalent domain integral approach*, Eng. Frac. Mech., 73(18): 2802-2828. doi: 10.1016/j.engfracmech.2006.04.015
13. Sharma, S., Yadav, S. (2013), *Thermo elastic-plastic analysis of rotating functionally graded stainless steel composite cylinder under internal and external pressure using finite difference method*, Adv. in Mater. Sci. & Eng. doi:10.1155/2013/810508
14. Seth, B.R. (1970), *Transition conditions: The yield condition*, Int. J Non-Linear Mech., 5(2): 279-285.
15. Sharma, S., Sahay, I., Kumar, R. (2012), *Creep transition in non homogeneous thick-walled circular cylinder under internal and external pressure*, Appl. Math. Sci., 6(122):6075-6080.
16. Sharma, S., Sahay, I., Kumar, R. (2014), *Thermo elastic-plastic transition of transversely isotropic thick-walled circular cylinder under internal and external pressure*, Multidis. Model. Mater. Struc., 10(2), 211-227. doi.org/10.1108/MMMS-03-2013-0026
17. Aggarwal, A.K., Sharma, R., Sharma, S. (2014), *Collapse pressure analysis of transversely isotropic thick-walled cylinder using Lebesgue strain measure and transition theory*, Scientif. World J, doi: 10.1155/2014/240954
18. Seth, B.R. (1966) *Measure concept in mechanics*, Int. J Non-Linear Mech., 1(1): 35-40.
19. Borah, B.N., (2005), *Thermo elastic plastic transition*, Contemporary Mathematics, 379: 93-111.
20. Sharma, S., (2017), *Stress analysis of elastic-plastic thick-walled cylindrical pressure vessels subjected to temperature*, Struc. Integ. and Life, 17(2): 105-112.
21. Sharma, S. (2017), *Creep transition in bending of functionally graded transversely isotropic rectangular plates*, Struc. Integ. and Life, 17(3): 187-192.

© 2018 The Author. Structural Integrity and Life, Published by DIVK (The Society for Structural Integrity and Life 'Prof. Dr Stojan Sedmak') (<http://divk.inovacionicentar.rs/ivk/home.html>). This is an open access article distributed under the terms and conditions of the [Creative Commons Attribution-NonCommercial-NoDerivatives 4.0 International License](#)

CALENDAR OF CONFERENCES, MEETINGS, CONGRESSES

October 28-31, 2018	IALCEE 2018 The Sixth International Symposium on Life-Cycle Civil Engineering	Ghent, Belgium	http://www.ialcce2018.org
November 24-28, 2018	GeoMEast 2018 – International Congress and Exhibition 'Sustainable Civil Infrastructures: Structural Integrity'	Cairo, Egypt	http://www.geomeast2018.org
March 27-29, 2019	IABSE Symposium Guimaraes Towards a Resilient Built Environment Risk and Asset Management (Annual Meetings precede the Conference)	Guimaraes, Portugal	http://www.iabse.org/guimaraes2019
June 24-26, 2019	12 th International Conference on Multiaxial Fatigue and Fracture (ICMFF12)	Bordeaux, France	link
July 24-26, 2019	ICSA 2019 - 4th International Conference on Structures and Architecture	Lisbon, Portugal	http://www.icsa2019.com
September 4-6, 2019	IABSE Congress 'The Evolving Metropolis' (Annual Meetings precede the Congress)	New York City, USA	http://www.iabse.org/newyork2019
October 2-4, 2019	ARCH 2019 - 9th International Conference on Arch Bridges	Porto, Portugal	http://www.fe.up.pt/arch19
March 30 - April 3, 2020	VAL4, 4 th International Conference on Material and Component Performance under Variable Amplitude Loading	Darmstad, Germany	First Announcement